Int. J. Nanosci. Nanotechnol., Vol. 16, No. 3, Sept. 2020, pp. 181-188

Study on Fe_3O_4 Magnetic Nanoparticles Size Effect on Temperature Distribution of Tumor in Hyperthermia: A Finite Element Method

Shahryar Malekie[1,*] and Ali Rajabi[2]

[1]Radiation Applications Research School, Nuclear Science and Technology Research Institute, PO Box 31485-498, Karaj, Iran.
[2]Secondary Standard Dosimetry Laboratory (SSDL), Pars Isotope, Karaj, Iran.

(*) Corresponding author: smaleki@aeoi.org.ir
(Received: 05 February 2019 and Accepted: 06 March 2020)

Abstract

In recent years, Hyperthermia has been used as an emerging technique for cancer treatment, especially for localized tumors. One of the promising cancer treatment approaches is magnetic nanoparticle (MNPs) Hyperthermia. In this theoretical work, the temperature distribution of a common tumor over the different sizes of Fe3O4 magnetic nanoparticles, namely 25, 50, 100, and 200 nm, was studied via the finite element method. A two-dimensional method was used to simulate the tumor tissue, in which nanoparticles were incorporated and dispersed into the tumor uniformly. The bio heat transfer equation (BHTE) was applied to calculate the thermal processes in the human body. Results elucidated that decreasing magnetic nanoparticle size caused more temperature rise in the tumor cell during the Hyperthermia treatment, which led to better performance of the treatment. Finally, simulation results showed that the Fe3O4 magnetic nanoparticles with the sizes of 50-100 nm were applicable for Hyperthermia therapy with the optimum cellular uptake.

Keywords: *Hyperthermia, Magnetic nanoparticles, Size effect, Tumor, Finite element method.*

1. INRODUCTION

In chemotherapy, generally below the 0.1% of the drugs are absorbed by tumors, while 99.9% delivering into the normal tissue [1]. Hyperthermia therapy refers to body temperatures enhanced to knock out cancer cells. It is always handled with other types of cancer therapy, e.g., chemotherapy and radiation therapy [2]. In Hyperthermia, various techniques attributing to different energies are used, including heat, microwave, laser, ultrasound, and magnetic fields [3]. One of the promising cancer treatment approaches is magnetic nanoparticle (MNPs) Hyperthermia. In fact, by injecting the MNPs such as Fe_3O_4 in the tumor and subjecting these nanoparticles into a changeable magnetic field, they generate heat, reaching to temperatures up to 42°C that probably cancer cells can be killed, commonly with the lowest damage to the healthy tissue [4]. Consequently, this approach can diminish tumors with negligible side effects [4]. The magnetic fields produced by Hyperthermia studies are limited to 70 mT [5] to 1.5 T [6, 7]. Iron oxide nanoparticles colloids peculiarly magnetite (Fe_3O_4) and maghemite (γ - Fe_2O_3) were studied for magnetic Hyperthermia because of their biocompatibility and high magnetization [8-12]. Several investigations have been carried out on Fe3O4 nanoparticles [13-15]. Mostly, these ferrofluid particles in the form of emulsion injected into a patient [1]. These MNPs have been examined in humans and

animals [16-19]. Several researchers investigated magnetic Hyperthermia [20-30].

The dissipation of the MNPs power in a hysteresis loop is introduced as a specific loss power (SLP) or specific absorption rate (SAR) [31]. Usually, three crucial procedures are taken into account for the heating features of the MNPs [31]. Firstly, Néel relaxation, in which the magnetization of the MNPs is provoked by thermal instabilities [31]. Secondly, Brownian relaxation regarding the rotation of the MNPs in the Brownian motion, and lastly, the external fields [31]. Several factors determine the mechanisms, as mentioned earlier, like the temperature, uniformity, and the frequency of the magnetic field, size, and saturation magnetization of the MNPs [31]. The size of the MNPs is an essential parameter in the magnetic particle Hyperthermia. Particle sizes of Fe_3O_4 nanoparticles can be manipulated by different production procedures ranging from nanometer to micrometer sizes [1, 32-34]. Thapa *et al*. reported a new method to fabricate the MNPs ranging from 5-100 nm [35]. In the other work, Hilger *et al*. investigated the breast adenocarcinoma cells embedded into immunodeficient mice via injection of the MNPs into the tumor cells regarding 6.5 kA/m magnetic field at a frequency of 400 kHz, in which exhibited temperature enhances up to 73°C in the tumor domains [36, 37].

In this theoretical work, the evaluation of the temperature distribution of a common tumor is investigated over the different sizes of Fe_3O_4 magnetic nanoparticles with uniform dispersion in the tumor via the finite element method considering the Hyperthermia approach.

1.1. Pennes Equation for Bio Heat Transfer (BHTE)

The equation related to heat transfer in a biomaterial is given by Pennes equation [38] :

$$\rho c\frac{\partial T}{\partial t} = \nabla\cdot(k\nabla T) + \sigma E^2 - c_b W_b (T - T_b) + Q_m \quad (1)$$

Where ρ, c, k, T, c_b, W_b, T_b, Q_m, and E are density, specific heat capacity, thermal conductivity, temperature, specific heat capacity of blood, blood mass flow rate, the temperature of blood, specific power and electric field respectively [39]; E is obtained via $E = -\nabla V$, where V is the electrical potential which is determined from the solving of the Laplace's equation ($\nabla^2 V = 0$) in the defined boundary conditions. As can be seen from the Fig. 1 , the blood mass flow rate or blood perfusion in the tumor can be calculated as [40]:

$$W_{tumor} = \begin{cases} 0.8 & T < 37 \\ 0.8 - \dfrac{(T-37)^{4.8}}{5400} & 37 \le T \le 42 \\ 0.38 & T > 42 \end{cases} \quad (2)$$

Since the blood mass flow rate in capillaries and tissues depends on their actual temperature, so as can be easily seen from the Fig. 1, it can be deduced that perfusion in tumor tissue in the range of 37-42 °C declines and reaches to its minimum value of 0.38 kg/(s.m^3) in 42°C, and after that despite temperature rise, but the value of perfusion remains constant.

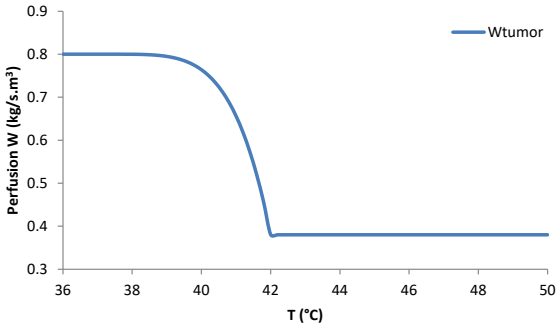

Figure 1. *Perfusion rate value in different temperatures for tumor tissue.*

Therefore, in Hyperthermia for curing the cancer cells, there is an optimum temperature that there is no need to increase the temperature of tumor tissue necessarily beyond it.

1.2 Magnetic Field and Heating Mechanism

Maxwell's equations are given by [1]:

$$\nabla \times \vec{H} = \vec{J} \quad (3)$$

$$\nabla \cdot \vec{B} = 0 \quad (4)$$

$$\vec{B} = \mu_0\left(\vec{H} + \vec{M}\right) = \mu_0\left(\vec{H} + \chi\vec{H}\right) = \mu_0\vec{H}(1+\chi) \quad (5)$$

In which $\vec{B}, \vec{H}, \vec{J}, \vec{M}$, *and* χ are the magnetic field, magnetic intensity, current density, magnetization, and magnetic susceptibility, respectively, while μ_0 is the permeability of the vacuum [1]. Due to the negligible amount of χ for human body ($\chi \approx 10^{-6} - 10^{-4}$), it is evident that the magnetic field can transmit in the body unchangeably [1]. While Fe_3O_4 nanoparticles exhibit higher magnetic susceptibilities ($\chi \approx 20$) [1]. The force applied to a magnetic nanoparticle is introduced as [1]:

$$\vec{F}_M = \frac{4\pi a^3}{3}\frac{\mu_0\chi}{1+\chi/3}\left[\frac{d\vec{H}}{d\vec{x}}\right]\vec{H} = \frac{2\pi a^3}{3}\frac{\mu_0\chi}{1+\chi/3}\nabla\left(\left|\vec{H}\right|^2\right) \quad (6)$$

which a is the radius of a nanoparticle. As can be seen from Fig. 2, the alignment of MNPs is affected by the applied magnetic field. The spatial orientation of the MNP is described by the respective polar and azimuthal angles of θ, ϕ, and magnetization relative to the applied field [41]. Usually, in Hyperthermia, the magnetic field is ranging from 70 mT [5] to 2.2 T [1, 42].

Diffusion coefficient of a tissue (D_B) exhibits an inverse relationship with the particle radius [1]:

$$D_B = \frac{k_B T}{6\pi\eta a} \quad (7)$$

which k_B, T ,a , and η are the Boltzmann constant, temperature, particle radius , and fluid viscosity [1].

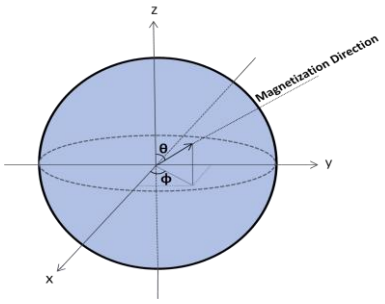

Figure 2. *The schematic view of a magnetic nanoparticle influenced by the magnetic force on its magnetization orientation.*

The value of produced heat per unit volume in a hysteresis process is given by [16]:

$$P = \mu_0 f \oint H\, dM \quad (8)$$

which, f is the frequency of the alternating magnetic field ranging from f=0.05-1.2 MHz and H=0-15 kA m^{-1} conventionally [16].

2. SIMULATION METHODOLOGY

2.1. Uniform Distribution of MNPs

This simulation considers dispersed MNPs of Fe_3O_4 with sizes of 25, 50, 100, and 200 nm in typical tumor tissue with an elliptical cross-section according to Fig. 3. For this purpose, we considered a 2D array of nanoparticles with a size of 4 μm×4 μm in which the number of nanoparticles was exhibited in Table 1 with a constant volume fraction of 7.4% in the tumor cell. The dispersion state of the MNPs of Fe_3O_4 in the tumor is such that these particles satisfy the excluded volume approach in order to prevent from the overlapping or penetration of nanoparticles to each other. In this simulation, an AC magnetic field was imported into the problem via the Pennes equation (Eq.1). It can be assumed that the specific power (Q_m) in the Eq.1 and the value of the produced heat per unit volume (P) in the Eq.8 are equivalent. Also P and Q_m have the same unit of W/m^3. Measurement of the Neel relaxation of magnetic particles in the frequency ranging from 1 kHz to 160 MHz was introduced by Fannin and et al. [43]. So, this simulation

was implemented for the case that f=100 kHz, H=4 kA/m, and $\chi = 20$. It can be calculated that from the Eq.5, B=105 mT, that is within the range of the other reported investigation [5]. In this simulation, $H \cdot f = 4.0 \times 10^8 Am^{-1}s^{-1}$ that satisfies the '*Atkinson-Brezovich criterion*' in which $H \cdot f = 4.85 \times 10^8 Am^{-1}s^{-1}$. This issue ensures the safe and tolerable amount of magnetic field applied for humans [4, 44]. The physical quantities have been exhibited in Table 2.

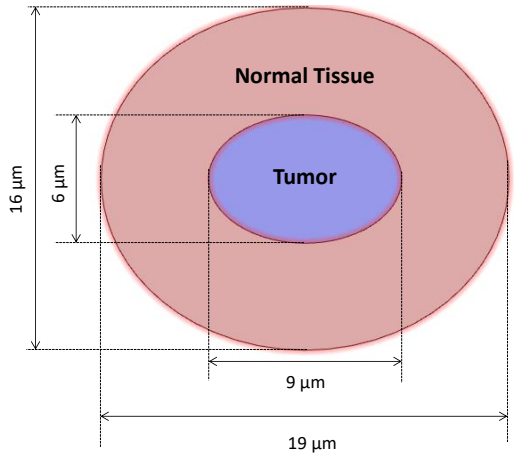

Figure 3. *Schematic view of the geometry in this model.*

Table 1*. The number of MNPs and their sizes in a square lattice.*

Array	Number of nanoparticles	r (nm)
5×5	25	200
10×10	100	100
20×20	400	50
40×40	1600	25

Table 2*. Physical quantities and their values in this simulation[45].*

Layer	Thermal Conductivity (W/m.K)	Heat Capacity (J/kg.K)	Density (kg/m^3)
Healthy Tissue	0.51	3760	1045
Tumor	0.51	3760	1045
Fe_3O_4	2000.6	644	5

2.2. Finite Element Method

The finite element method (FEM) is a robust numerical technique for solving boundary-value problems (BVPs) [46]. In FEM, the domain is divided into small subdomains or elements, which are related to each other by the nodes [47]. During Hyperthermia therapy, finding the precise answer of the BHTE for a tumor tissue is a challenging issue, so FEM can be useful to obtain the temperature distribution in the tumor tissue. A schematic exhibition of 2D mesh processing of this simulation is depicted in Fig. 4. In order to find the electrical potential of the elements, the Laplace equation was solved. In this simulation, a personal computer having 32 GB RAM and 3.4 GHz processor was used to predict the temperature distribution in tumor tissue numerically.

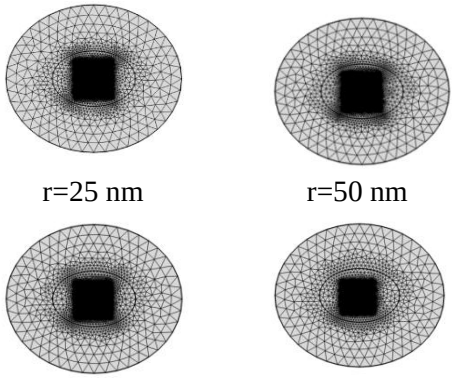

Figure 4. *Mesh quality simulated in this research.*

3. RESULTS AND DISCUSSION

Fig. 5 plots the thermal distribution in healthy tissue and tumor for the Fe_3O_4 MNPs with different sizes. Considering Fig. 5, the amount of normal tissue temperature remains constant at 37°C, while the temperature of the tumor domain increases with the decrease of the MNP size.

According to Table 3, it can be concluded that decreasing MNP size resulted in a temperature rise in the tumor cell during the Hyperthermia treatment. As can be easily seen from Table 3, the maximum temperature in the tumor cell is

related to the minimum nanoparticle size of 25 nm. To justification of this phenomenon, it can be mentioned those small size particles due to 25 nm exhibit a more massive amount of surface to volume ratio; thus, the significant discrepancy between thermal conductivities of tissue and the Fe_3O_4 MNPs results in increasing the temperature in the tumor tissue.

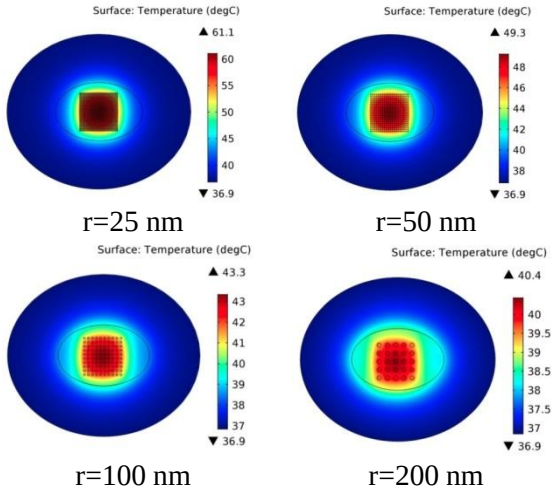

Figure 5. *Thermal distribution of Fe3O4 MNPs with different sizes in healthy tissue and tumor.*

Also, 'Brownian rotation' of the MNPs causes to increase the temperature in the tumor region [16].

Maybe the higher temperature rise due to smaller particle sizes is related to a more considerable amount of 'Brownian rotation' for small particles or lower amount of rotational inertia of the MNP, regarding the fact that rotational inertia of a body is equal to the product of mass and square of the distance of the object to the rotation axis. The moment of inertia for nanoparticles can be calculated using the standard definition in mechanics [48]. It can be mentioned that small particles with sizes up to 25 nm generally present superparamagnetic mode that stimulates a reduction in the agglomeration when the magnetic fields are eliminated [1].

It should be considered a compromise between the size of the MNPs and the maximum temperature rise in the tumor. Several related experiments [49, 50], and simulations [51-54], about the magnetic nanoparticles with different sizes for Hyperthermia have been reported.

As can be easily seen from Fig. 1, there is an optimum temperature that there is no need to increase the temperature of tumor tissue necessarily beyond it, so decreasing the MNPs size or increasing the maximum temperature in tumor cells subsequently is not adequate.

For larger nanoparticles more than 100 nm, the cellular uptake is decreased because of the larger nanoparticles unable to diffuse into the tumor cells quickly. Regarding this fact, it can be mentioned that the MNPs with the sizes of 50-100 nm are practical for Hyperthermia therapy.

Table 3. *The maximum temperature in tumor tissue for different sizes of MNPs.*

Magnetic nanoparticle radius (nm)	Maximum temperature in the tumor (°C)	Temperature rise [1] ΔT (°C)
25	61	24
50	49	12
100	43	6
200	41	4

[1] The thermal difference between normal (37°C) and tumor tissues

4. CONCLUSION

In summary, the temperature distribution of a common tumor over the different sizes of Fe_3O_4 MNPs, namely 25, 50, 100, and 200 nm were studied regarding the finite element procedure. A two-dimensional method was used to simulate the tumor tissue, in which nanoparticles were incorporated and dispersed into the tumor uniformly. The bio heat transfer equation was applied to calculate the thermal processes in the human body. Results showed that decreasing of magnetic nanoparticle size caused to temperature rise in the tumor cell during the Hyperthermia treatment or better performance of the treatment. One of the benefits of this method is that the temperature of the healthy tissue remains constant at 37°C, and only the temperature of the tumor domain is increased by

incorporating the magnetic nanoparticles into the tumor. Regarding this fact, it can be mentioned that the magnetic nanoparticles of Fe_3O_4 with the sizes of 50-100 nm are practical for Hyperthermia therapy with the optimum cellular uptake.

Conflicts of Interest

The authors declare that there are no conflicts of interest regarding this article.

REFERENCES

1. Nacev, A. N., (2013). "*Magnetic drug targeting developing the basics*", Department of Bioengineering, University of Maryland.
2. Wust, P., Hildebrandt, B., Sreenivasa, G., Rau, B., Gellermann, J., Riess, H., Felix, R., Schlag, P. (2002). "Hyperthermia in combined treatment of cancer", *The lancet oncology*, 3: 487-497.
3. Van der Zee, J., (2002). "Heating the patient: a promising approach?", *Ann. Oncol.*, 13: 1173-1184.
4. Vasilakaki, M., Binns, C., Trohidou, K. N., (2002). "Susceptibility losses in heating of magnetic core/shell nanoparticles for hyperthermia: a Monte Carlo study of shape and size effects", *Nanoscale*, 7: 7753-7762.
5. Holligan, D., Gillies, G., Dailey, J., (2003). "Magnetic guidance of ferrofluidic nanoparticles in an in vitro model of intraocular retinal repair", *Nanot*, 14: 661.
6. Ganguly, R., Gaind, A. P., Sen, S., Puri, I. K., (2005). "Analyzing ferrofluid transport for magnetic drug targeting", *J. Magn. Magn. Mater.*, 289: 331-334.
7. Jurgons, R., Seliger, C., Hilpert, A., Trahms, L., Odenbach, S., Alexiou, C., (2005). "Drug loaded magnetic nanoparticles for cancer therapy", *J. Phys.: Condens. Matter*, 18: S2893.
8. Kallumadil, M., Tada, M., Nakagawa, T., Abe, M., Southern, P., Pankhurst, Q. A., (2009). "Corrigendum to Suitability of commercial colloids for magnetic hyperthermia"[J. Magn. Magn. Mater. 321: 1509-1513], *J. Magn. Magn. Mater.*, 321: 3650-3651.
9. Laurent, S., Dutz, S., Häfeli, U. O., Mahmoudi, M., (2011). "Magnetic fluid hyperthermia: focus on superparamagnetic iron oxide nanoparticles", *Adv. Colloid Interface Sci.*, 166: 8-23.
10. Fortin, J. P., Wilhelm, C., Servais, J., Ménager, C., Bacri, J. C., Gazeau, F., (2007). "Size-sorted anionic iron oxide nanomagnets as colloidal mediators for magnetic hyperthermia", *J. Am. Chem. Soc*, 129: 2628-2635.
11. Chen, R., Christiansen, M. G., Anikeeva, P., (2013). "Maximizing hysteretic losses in magnetic ferrite nanoparticles via model-driven synthesis and materials optimization", *ACS nano*, 7: 8990-9000.
12. Basti, H., Hanini, A., Levy, M., Tahar, L. B., Herbst, F., Smiri, L. S., Kacem, K., Gavard, J., Wilhelm, C., Gazeau, F., Chau, F., Ammar, S., (2014). "Size tuned polyol-made Zn 0.9 M 0.1 Fe 2 O 4 (M = Mn, Co, Ni) ferrite nanoparticles as potential heating agents for magnetic hyperthermia: from synthesis control to toxicity survey*", Materials Research Express*, 1: 045047.
13. Hatamzadeh, M., Johari-Ahar, M., Jaymand, M., (2012). "In situ chemical oxidative graft polymerization of aniline from Fe3O4 nanoparticles", *International Journal of Nanoscience and Nanotechnology*, 8: 51-60.
14. Khan, S., Pathak, B., Fulekar, M., (2017). "Spherical Surfaced Magnetic (Fe3O4) Nanoparticles as Nano Adsorbent Material for Treatment of Industrial Dye Effluents", *International Journal of Nanoscience Nanotechnology*, 13: 169-175.
15. Banisharif, A., Hakim Elahi, S. Anaraki Firooz, A., Khodadadi, A. A, Mortazavi, Y., (2013). "TiO2/Fe3O4 nanocomposite photocatalysts for enhanced photo-decolorization of congo red dye", *International Journal of Nanoscience and Nanotechnology*, 9: 193-202.
16. Pankhurst, Q. A., Connolly, J., Jones, S. K., Dobson, J., (2003). "Applications of magnetic nanoparticles in biomedicine", *J. Phys. D: Appl. Phys.*, 36: R167.
17. Pankhurst, Q. A., Thanh, N. T. K, Jones, S. K., Dobson, J., (2009). "Progress in applications of magnetic nanoparticles in biomedicine", *J. Phys. D: Appl. Phys.*, 42: 224001.
18. Mahmoudi, M., Serpooshan, V., Laurent, S. (2011). "Engineered nanoparticles for biomolecular imaging", *Nanoscale*, 3: 3007-3026.
19. Krukemeyer, M. G., Krenn, V., Jakobs, M., Wagner, W., (2012). "Mitoxantrone-iron oxide biodistribution in blood, tumor, spleen, and liver—magnetic nanoparticles in cancer treatment", *J. Surg. Res.*, 175: 35-43.
20. Zhu, L., Zhou, Z., Mao, H., Yang, L., (2017). "Magnetic nanoparticles for precision oncology: theranostic magnetic iron oxide nanoparticles for image-guided and targeted cancer therapy", *Nanomedicine*, 12: 73-87.
21. Gutierrez-Guzman, D., Lizardi, L., Otálora, J., Landeros, P., (2017). "Hyperthermia in low aspect-ratio magnetic nanotubes for biomedical applications", *Appl. Phys. Lett.*, 110: 133702.

22. LeBrun, A., Joglekar, T., Bieberich, C., Ma, R., Zhu, L., (2017). "Treatment Efficacy for Validating MicroCT-Based Theoretical Simulation Approach in Magnetic Nanoparticle Hyperthermia for Cancer Treatment", *J. Heat Transfer*, 139: 051101.
23. Fang, C. H., Tsai, P. I., Huang, S. W., Sun, J. S., Chang, J. Z. C., Shen, H. H., Chen, S. Y., Lin, F. H., Hsu, L. T., Chen, Y. C., (2017). "Magnetic hyperthermia enhance the treatment efficacy of peri-implant osteomyelitis", *BMC Infect. Dis.*, 17: 516.
24. Shabestari Khiabani, S., M. Farshbaf, A. Akbarzadeh, S. Davaran, (2017). "Magnetic nanoparticles: preparation methods, applications in cancer diagnosis and cancer therapy", *Artificial cells, nanomedicine, and biotechnology*, 45:6-17.
25. Hoopes, P. J., Moodie, K. L., Petryk, A. A., Petryk, J. D., Sechrist, S., Gladstone, D. J., Steinmetz, N. F., Veliz, F. A., Bursey, A. A., Wagner, R. J., (2017). "*Hypo-fractionated radiation, magnetic nanoparticle hyperthermia and a viral immunotherapy treatment of spontaneous canine cancer*", Energy-based Treatment of Tissue and Assessment IX, International Society for Optics and Photonics, 1006605.
26. Dutz, S., Hergt, R., (2014). "Magnetic particle hyperthermia—a promising tumour therapy?", *Nanot*, 25: 452001.
27. Yi, G. q., Gu, B., Chen, L. k., (2014). "The safety and efficacy of magnetic nano-iron hyperthermia therapy on rat brain glioma", *Tumour Biol*., 35: 2445-2449.
28. Asín, L., Ibarra, M., Tres, A., Goya, G., (2012). "Controlled cell death by magnetic hyperthermia: effects of exposure time, field amplitude, and nanoparticle concentration", *Pharm. Res.*, 29: 1319-1327.
29. Balivada, S., Rachakatla, R. S., Wang, H., Samarakoon, T. N., Dani, R. K., Pyle, M., Kroh, F. O., Walker, B., Leaym, X., Koper, O. B., (2010). "A/C magnetic hyperthermia of melanoma mediated by iron (0)/iron oxide core/shell magnetic nanoparticles: a mouse study", *BMC Cancer*, 10:119.
30. Hergt, R., Dutz, S., Müller, R., Zeisberger, M., (2006). "Magnetic particle hyperthermia: nanoparticle magnetism and materials development for cancer therapy*", J. Phys.: Condens. Matter*, 18: S2919.
31. Harabech, M., Leliaert, J., Coene, A., Crevecoeur, Van Roost, G. D., Dupré, L., (2017). "The effect of the magnetic nanoparticle's size dependence of the relaxation time constant on the specific loss power of magnetic nanoparticle hyperthermia", *J. Magn. Magn. Mater.*, 426: 206-210.
32. Figuerola, A., Corato, R.I., Manna, L., Pellegrino, T., (2010). "From Iron Oxide Nanoparticles towards Advanced Iron-Based Inorganic Materials Designed for Biomedical Applications", *Pharmacol. Res.*, 62: 126-143.
33. Veiseh, O., Gunn, J., Zhang, M., (2010). "Design and fabrication of magnetic nanoparticles for targeted drug delivery and imaging", *Adv. Drug Deliv. Rev.*, 62: 284–304.
34. Sun, C., Lee, J., Zhang, M., (2008). "Magnetic nanoparticles in MR imaging and drug delivery", *Adv. Drug Deliv. Rev.* , 60: 1252–1265.
35. Thapa, D., Palkar, V., Kurup, M., Malik, S., (2004). "Properties of magnetite nanoparticles synthesized through a novel chemical route", *Mater. Lett.*, 58: 2692-2694.
36. Hilger, I., Hiergeist, R., Hergt, R., Winnefeld, K., Schubert, H., Kaiser, W. A., (2002). "Thermal ablation of tumors using magnetic nanoparticles: an in vivo feasibility study", *Invest. Radiol.*, 37: 580-586.
37. Giustini, A. J., Petryk, A. A., Cassim, S. M., Tate, J. A., Baker, I., Hoopes, P. J., (2010). "*Magnetic nanoparticle hyperthermia in cancer treatment*", Nano Life, 1: 17-32.
38. Pennes, H. H., (1948). "Analysis of tissue and arterial blood temperatures in the resting human forearm", *J. Appl. Physiol.*, 1: 93-122.
39. Ambrosio, V. D., Dughiero, F., (2007). "Numerical model for RF capacitive regional deep hyperthermia in pelvic tumors", *Med Bio Eng Comput*, 45: 459-466.
40. Tompkins, D., Vanderby, R., Klein, S., Beckman, W., Steeves, R., Frye, D., Paliwal, B., (1994). "*Temperature-dependent versus constant-rate blood perfusion modelling in ferromagnetic thermoseed hyperthermia: results with a model of the human prostate*", International journal of hyperthermia: the official journal of European Society for Hyperthermic Oncology, North American Hyperthermia Group, 10: 517-536.
41. Skomski, R., Balamurugan, B., Manchanda, P., Chipara, M., Sellmyer, D.J., (2017). "Size Dependence of Nanoparticle Magnetization", *IEEE Trans. Magn.*, 53.
42. Alexiou, C., Diehl, D., Henninger, P., Iro, H., Rockelein, R., Schmidt, W., Weber, H., (2006). "A high field gradient magnet for magnetic drug targeting", *ITAS*, 16:1527-1530.
43. Fannin, P., (1991). "Measurement of the Neel relaxation of magnetic particles in the frequency range 1 kHz to 160 MHz", *J. Phys. D: Appl. Phys.*, 24: 76.
44. Atkinson, W. J., Brezovich, I. A., Chakraborty, D.P., (1984). "Usable frequencies in hyperthermia with thermal seeds", *IEEE Trans. Biomed. Eng.*, 70-75.

45. Callister, W. D., (2001). "*Fundamentals of Materials Science and Engineering*", fifth ed., John Wiley & Sons, Inc., The University of Utah.
46. Reddy, J., (2005). "*An introduction to the finite element method*", 3rd ed., MC Graw-Hill Series in Mechanical Engineering.
47. Malekie, S., Ziaie, F., (2017). "A two-dimensional simulation to predict the electrical behavior of carbon nanotube/polymer composites", *J. Polym. Eng.*, 37: 205-210.
48. Wang, Z. L., Gao, R. P., Pan, Z. W., Dai, Z. R., (2001). "Nano-scale mechanics of nanotubes, nanowires, and nanobelts", *Adv. Eng. Mater.*, 3: 657.
49. Guo, X., Wu, Z., Li, W., Wang, Z., Li, Q., Kong, F., Zhang, H., Zhu, X., Du, Y.P., Jin, Y., (2016). "Appropriate size of magnetic nanoparticles for various bioapplications in cancer diagnostics and therapy", *ACS Applied Materials & Interfaces*, 8: 3092-3106.
50. Ovejero, J. G., Cabrera, D., Carrey, J., Valdivielso, T., Salas, G., Teran, F. J., (2016). "Effects of inter-and intra-aggregate magnetic dipolar interactions on the magnetic heating efficiency of iron oxide nanoparticles", *PCCP*, 18: 10954-10963.
51. Rajabi, A., Malekie, S., (2017). "*Simulation of magnetic nanoparticle hyperthermia for curing the tumors using finite element method*", Secon Nanomedicine and Nanosafety Conference (NMNS 2017), Tehran University of Medical Sciences.
52. Valente, A., Loureiro, F., Di Bartolo, L., Mansur, W. J., (2018). "Computer simulation of hyperthermia with nanoparticles using an OcTree finite volume technique", *International Communications in Heat Mass Transfer*, 91: 248-255.
53. Taloub, S., Hobar, F., Astefanoaei, I., Dumitru, I., Caltun, O. F., (2016). "FEM Investigation of coated magnetic nanoparticles for hyperthermia", *Nanoscience and Nanotechnology*, 6: 55-61.
54. Dahwi, A. A., (2017). "Finite Element Simulation, Characterization and Transportation of Magnetic Nanoparticles under the Impact of Magnetic Field in Blood Vessels", *Global Journal of Pure Applied Mathematics*, 13: 7771-7784.